DYNAMIC BEHAVIOR OF PILE FOUNDATION DURING EARTHQUAKES

Y. Abe (I), M. Sugimoto (I), N. Ohki (II), Y. Suzuki (II),
J. Jido (II), Y. Hayamizu (II) and T. Hiromatsu (II)
Presenting Author: Y. Abe

SUMMARY

For the purpose of understanding soil-pile-building interaction and the dynamic behavior of piles during earthquakes, an earthquake observation has been carried out for an actual pile-supported building by using accelerometers and strain gauges since March, 1982. Out of many records obtained hitherto, those for several large earthquakes were analyzed. As a result, some interesting phenomena were confirmed with regard to amplification characteristics of soft subsoil, soil-pile-building interaction and strain distribution of piles.

INTRODUCTION

Since the 1968 Off-Tokachi Earthquake and the 1978 Off-Miyagi-Pref. Earthquake inflicted serious damage to pile foundations, it has become one of important studies to understand the dynamic behavior of a pile foundation during earthquakes.

The authors have been carring out the earthquake observation since 1975, so as to grasp the dynamic characteristics of soft alluvial ground (Ref. 1). However, a pile-supported building was constructed near the observation site. Therefore, the purpose of observation was switched to understanding soil-pile-building interaction and the dynamic behavior of piles during earthquakes, starting a new series of earthquake observations. With the progress of the building construction, the horizontal loading test of piles and the forced vibration test of the building were made. In addition to the previously installed underground accelerometers, many accelerometers and strain gauges were installed within the building and the piles. The new observation was started in March, 1982.

In one and a half years since the start of new observation, more than 40 earthquake records have been obtained. The spectrum analysis was made for several large records out of them. Some interesting results were obtained with regard to the soil-pile-building interaction and dynamic behavior of piles. This paper presents these results together with those of the horizontal loading test and forced vibration test.

OUTLINE OF GROUND, PILE, BUILDING AND OBSERVATION SYSTEM

The building to be observed is located at the site of our laboratory in the downtown Tokyo. The ground is composed, from the surface, of earth filling, alluvial sand, soft silt, alluvial clay and diluvial sand layer, as

(I) Research Engineer, Takenaka Technical Research Laboratory, Tokyo, Japan

(II) Chief Research Engineer, Ditto.

shown in the soil profile of Fig. 1. The shear wave velocity in each layer is 100 - 200 m/sec in silt, 300 m/sec in alluvial clay and 360 m/sec in diluvial sand. The building is a 2-story reinforced concrete rigid frame structure as shown in Fig. 1, supported in the diluvial sand layer at the depth of GL-45 m by cast-in-place concrete pile foundations of 1.0 m or 1.1 m in diameter.

The measuring instruments involve servo-type accelerometers (natural frequency f_o = 3 - 5 Hz) and gauge-type strainmeters. As shown in Fig. 1, 3 accelerometers are installed underground (G1 - G3), 2 in the building (B1, B2) and 2 in the P1 pile (F1, F2). Seven pairs of strain gauges are installed in the P1 pile (S1 - S7) and 4 pairs in the neighboring P2 pile (S1 - S4). As an earthquake occurs, principal 16 components of the accelerometer and 16 components of the strain gauge out of total 51 components are recorded on the magnetic tape by the digital data recorder (Ref. 2).

HORIZONTAL LOADING TEST OF PILE AND FORCED VIBRATION TEST OF BUILDING

For the purpose of obtaining reference data to check the strain distribution of pile during earthquakes, the horizontal loading test of the P1 pile was made. The alternating load was applied to the head of a pile, increasing to maximum load of 16 tons. As a part of the results, the bending moment distribution calculated from a pair of strains A and B (refer to the section of pile in Fig. 1) is shown by a dotted line in Fig. 2. The solid line in Fig. 2 represents the result of a simulation analysis based on the elastic beam theory in consideration of non-linearity of soil and pile. Two curves coincided well, indicating the validity of the analytic method and assumed conditions (Ref. 2). The bending moment distribution with the pile head fixed was calculated by using this analytic method. This condition of "pile head fixed" is supposed to be close to that of the pile head after the completion of the building. The result is shown in Fig. 3.

In order to understand the dynamic characteristics of the soil-pile-building interaction system, the sinusoidal forced vibration test was conducted after the completion of the building. The vibration generator was installed at the roof, and the vibration was applied in the transversal direction of the building (EW direction). The vibration frequency ranged from 1 Hz to 19 Hz, at 0.5 Hz frequency intervals. One of the results is shown in Figs. 4 and 5. Fig. 4 represents resonance curves at the roof (B1) and the first floor (B2), showing the response displacement for unit vibration force. The displacement of B1 is several times as large as that of B2, giving peak values at the frequencies of 5.5 Hz, 8.0 Hz and 9.5 Hz. Fig. 5 shows the resonance mode at each measuring point for a resonance frequency of 5.5 Hz. The thick solid line represents the mode shape when B1 gives maximum displacement. At this frequency, the P1 pile is vibrating in the mode of higher order. The mode shape of pile strain is symmetric in A and B series, indicating that bending deformation is dominant.

EARTHQUAKE OBSERVATION OF SOIL-PILE-BUILDING

The earthquake observation of the soil-pile-building interaction system was started when the building was completed in March 1982. In one and a half

years to September 1983, more than 40 earthquake motions were recorded. Among these earthquakes, 9 earthquakes shown in Table 1 exceeded degree III on the seismic intensity of J.M.A in Tokyo. The maximum acceleration on the first floor (B2) in No. 33 earthquake was the greatest, attaining to 75 gal. The maximum value distribution of EW components in these earthquakes is shown in Fig. 6. The strain distribution of the pile is shown for A series of the P1 pile. Both acceleration and strain are greatly amplified in the shallow layer. In the subsequent analyses, EW components of 5 earthquakes, Nos. 11, 16, 30, 32 and 33, were dealt with.

In order to examine the amplification characteristics of soft subsoil above the diluvial sand layer, the Fourier spectrum ratio of G1 to G3 (G1/G3) was calculated. The results are shown in Fig. 7 (a). The average of Fourier spectrum ratio as obtained before the construction of building is shown in Fig. 7 (b), so as to be compared with Fig. 7 (a). No significant difference was recognized in the predominant frequency between before and after construction of the building. Excepting the No. 30 earthquake (with the seismic center below Tokyo), the greater the maximum acceleration, the lower the predominant frequency of the first order tended to become, suggesting the nonlinearity of strain-dependency of soft subsoil.

In order to check the soil-pile-building interaction, the Fourier spectrum ratios B1/G3 and B2/G1' were calculated, where G1' denoted a free field point far from the building. The point G1' did not exist actually, and the spectrum ratio B2/G1' was calculated using the average amplification characteristics of ground before construction of the building (refer to Fig. 7 (b)). The calculated spectrum ratios B1/G3 and B2/G1' are shown in Figs. 8 and 9, respectively. The predominant frequency of B1/G3 was slightly lower than that of G1/G3 in every earthquake. The spectrum ratio B2/G1' had marked dips at the frequencies of 5.1 Hz, 6.6 Hz and 8.7 Hz in every earthquake. The presence of these dips indicates one of the effects of soil-pile-building interaction.

STRAIN OF PILE DURING EARTHQUAKES

As an example, the dynamic strain waveforms of the P1 pile in No. 33 earthquake are shown in Fig. 10. These figures show the records of a pair of strain gauges A and B at each point S1 and S6. The waveforms of bending strain (A-B)/2 and axial strain (A+B)/2 are also shown in Fig. 10. At the pile head S1, A and B waves are antiphase to each other in all duration time, showing that the bending strain prevails. On the other hand, at the intermediate depth S6, two waves become in-phase as the principal motion is passed over, that is, the axial strain prevails. The synthesized axial strain waves at S1 and S6 are nearly identical in respect of amplitude and waveform.

The distribution of maximum bending strain and axial strain of the P1 pile are shown in Fig. 11. These maximum values are normalized by the maximum acceleration of the EW component at the first floor B2 (refer to Table 1). The maximum bending strain is the greatest at the pile head, and becomes smaller as the depth increases. The distribution in No. 33 earthquake is somewhat different from that in other earthquakes. The maximum axial strain is uniform everywhere in the direction of depth, indicating the characteristics of the bearing pile. It is interesting that the maximum

axial strain in No. 11 earthquake, having the seismic center in the shallow layer far from the site, is greater than that in other earthquakes.

VIBRATION MODE OF PILE DURING EARTHQUAKES

In order to examine the relationship between the behavior of ground and that of a pile during earthquakes, the vibration modes of acceleration and strain were calculated in No. 33 earthquake, as shown in Fig. 12. These were calculated by means of passing through a narrow band filter. Each frequency of the band pass filter was selected considering predominant frequency of the soil-pile-building system (refer to Fig. 8). These modes are normalized by acceleration at the first floor B2, and the thick solid line represents the mode shape when B1 gives a maximum value. As shown in Fig. 12, at the frequencies of 0.9 Hz and 4.3 Hz, the pile and building are vibrating in-phase together with the ground, with the first and the third order mode, respectively. The building is vibrating as a rigid body at the first order mode, while the third order mode is supposed to involve the rocking component of the building.

The vibration mode of A strain series of the P1 pile in each earthquake is shown in Figs. 13 (a) and (b). Fig. 13 (c) shows the results of above-mentioned tests. The solid line shows the simulated distribution of bending moment with the pile head fixed (refer to Fig. 3), and the dashed line shows the resonance mode shape of the forced vibration test (refer to Fig. 5). From these figures, the following statements may be claimed: i) the first order mode is of a similar shape to each other, while the amplitude varies in different earthquakes, ii) the third order mode is nearly identical in various earthquakes in respect of amplitude and shape, and iii) the third order mode is in close resemblance to the distribution in Fig. 13 (c).

CONCLUSION

The earthquake observation has been conducted for an actual pile-supported building. The following points are concluded through the spectrum analyses of several records.

i) The predominant frequency of the ground is nearly identical between before and after construction of the building.
ii) The greater the maximum acceleration, the further shifts the predominant frequency of the ground toward lower frequency side, suggesting the non-linearity of strain-dependency of soft subsoil.
iii) In different earthquakes, there are some frequencies at which the earthquake motions at the first floor of a building are smaller than those on the free field far from the building.
iv) While bending strain is dominant at the pile head, it is of nearly identical magnitude to axial strain at the deeper position of the pile.
v) The maximum value of axial strain is nearly uniform in the direction of depth in every earthquake, and its waveform is of nearly the same shape regardless of depth.
vi) At the lower order mode, the pile-building is vibrating in-phase with the ground.
vii) The third order mode of a pile corresponds well to the distribution of bending moment of the pile with the head fixed as obtained by the simulation analysis of the horizontal loading test of the pile, and to the

resonance mode in the forced vibration test of the building.

These results have been confirmed by several records obtained hitherto with maximum acceleration not so large. It is expected that the general applicability of these phenomena would be proved through the accumulation of records in continued observations. Some of the records obtained by this observation are to be used for various simulation analyses by the members of the Subcommittee of Architectural Institute of Japan on Soil-Foundation Interaction (chairman: Prof. H. Kishida of Tokyo Institute of Technology). It is expected that the authors will participate in the simulation analysis as members of the subcommittee.

REFERENCES

1. Y. Abe and M. Sugimoto (1979): 'Earthquake Observation of Soft Subsoil', Proc. Annual Meeting of A.I.J, pp. 417 - 420, (in Japanese).
2. Y. Abe et al. (1982): 'Earthquake Observation of Soil-Pile-Structure', Proc. 6th Japan Earthquake Engineering Symposium, pp. 1545 - 1552, (in Japanese).

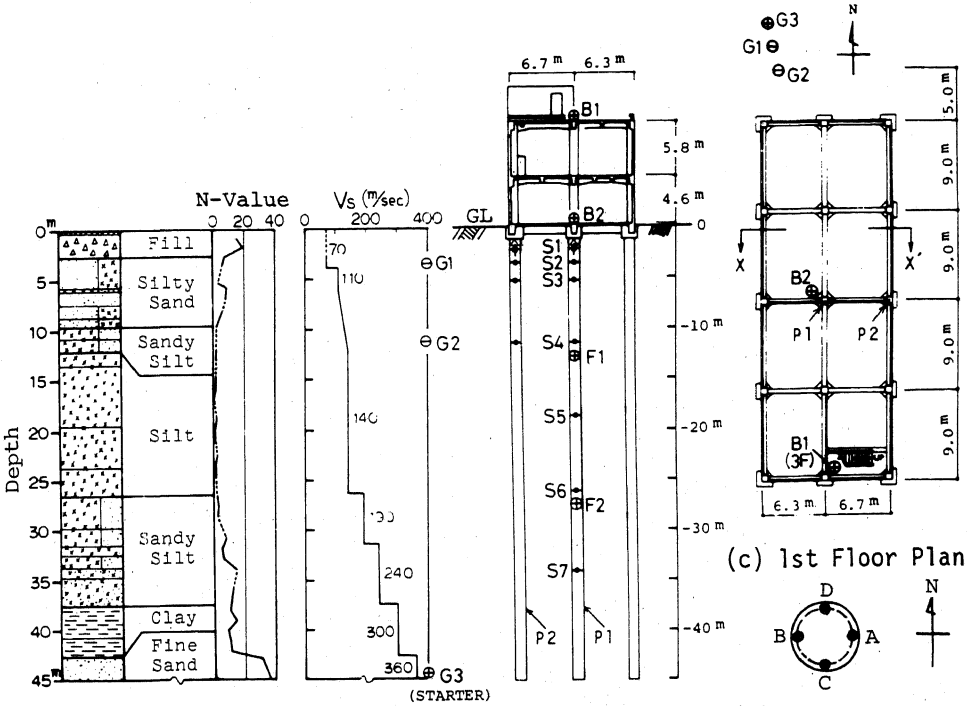

Fig.1 Outline of Ground, Pile & Building and Location of Transducers

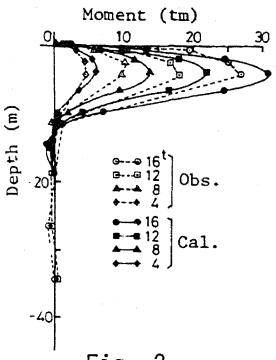

Fig. 2 Bending Moment Distribution (Horizontal Loading Test of Pl-pile)

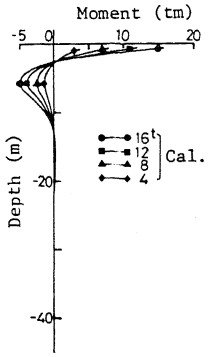

Fig. 3 Calculated Bending Moment Distribution (Pl-pile with its Head Fixed)

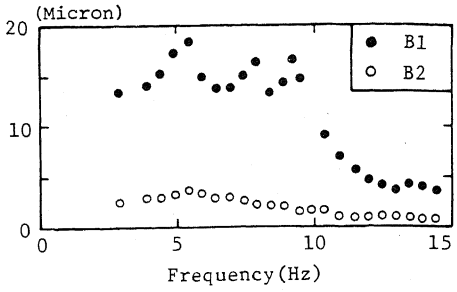

Fig. 4 Resonance Curve of Forced Vibration Test (EW-comp. Displacement)

Table 1 List of Earthquake

No.	Date	Epicenter	Mag. M	Depth (km)	Dist. (km)	Max. Acc. (gal) 1F-EW	Int. at Tokyo
2	1982. 3.19	Central Chiba Pref.	4.8	70	40	7.0	III
11	1982. 7.23	Off Ibaragi Pref.	7.0	10	200	23.6	III
16	1982. 8.12	Near of Izu-oshima Is.	5.7	40	90	15.9	IV
30	1983. 1.27	Easter Tokyo	4.6	60	20	11.4	III
32	1983. 2.22	Northern Chiba Pref.	4.9	80	25	13.3	III
33	1983. 2.27	Southern Ibaragi Pref.	6.0	70	40	75.3	IV
38	1983. 5.21	East off Chiba Pref.	5.2	30	70	4.6	III
43	1983. 7. 2	Off Fukushima Pref.	5.8	50	180	8.3	III
45	1983. 8. 8	Border of Kanagawa Pref. and Yamanashi Pref.	6.0	20	75	20.8	IV

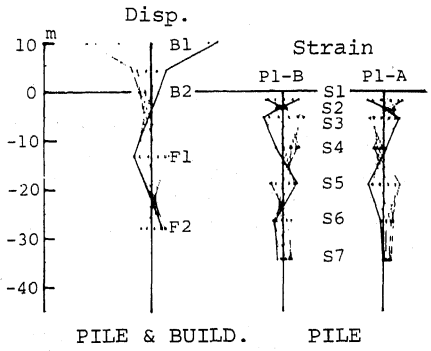

Fig. 5 Mode Shape of Forced Vibration Test (EW-comp. f=5.5 Hz)

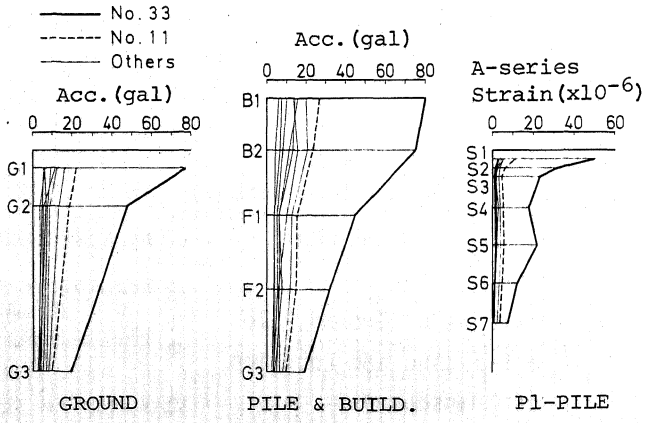

Fig. 6 Maximum Value Distribution (EW-comp.)

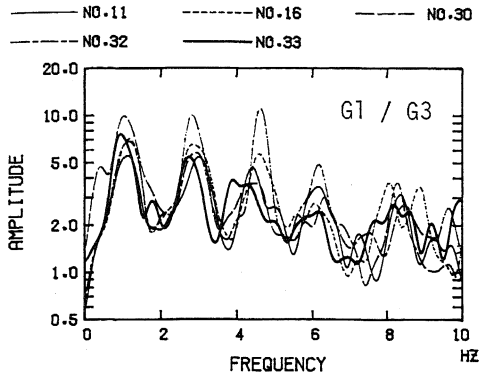

Fig. 7(a) Fourier Spectrum Ratio of G1 to G3 (After Construction)

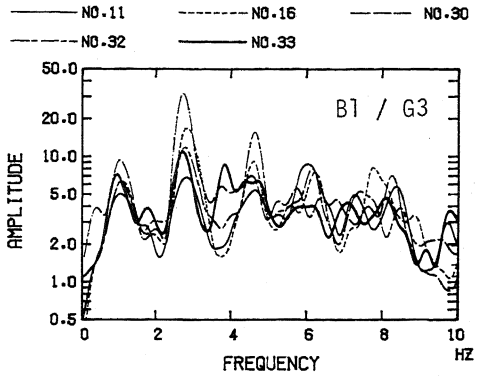

Fig. 8 Fourier Spectrum Ratio of B1 to G3

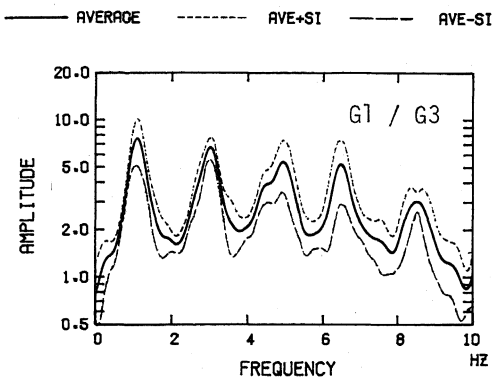

Fig. 7(b) Averaged Fourier Spectrum Ratio of G1 to G3 (Before Construction)

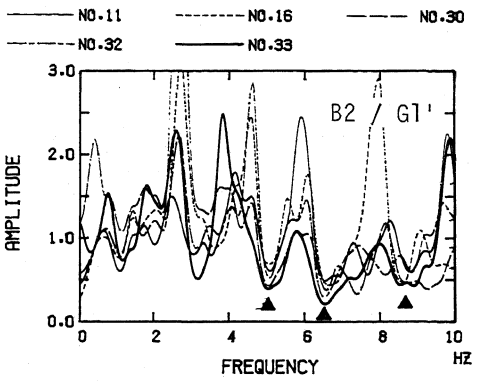

Fig. 9 Fourier Spectrum Ratio of B2 to G1'

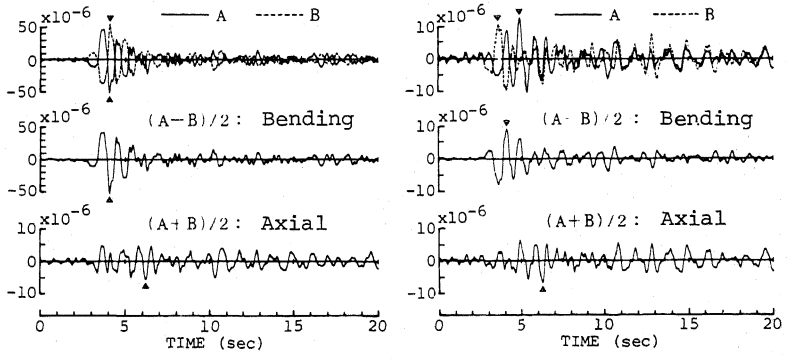

(a) Point S1 (b) Point S6

Fig. 10 Strain Wave of P1-pile (No.33 Earthquake)

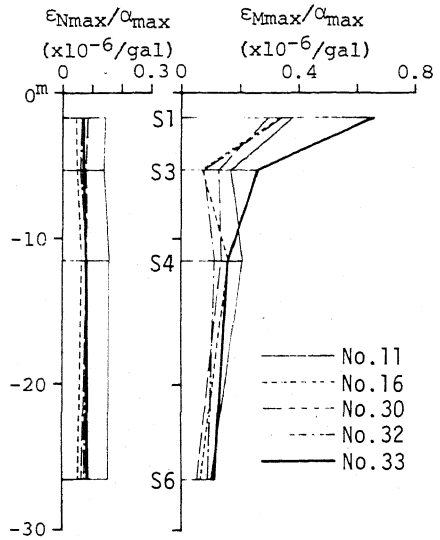

(a) Axial (b) Bending

Fig. 11 Maximum Strain Distribution of Pl-pile (Normalized by EW-comp. Max. Acc. of B2)

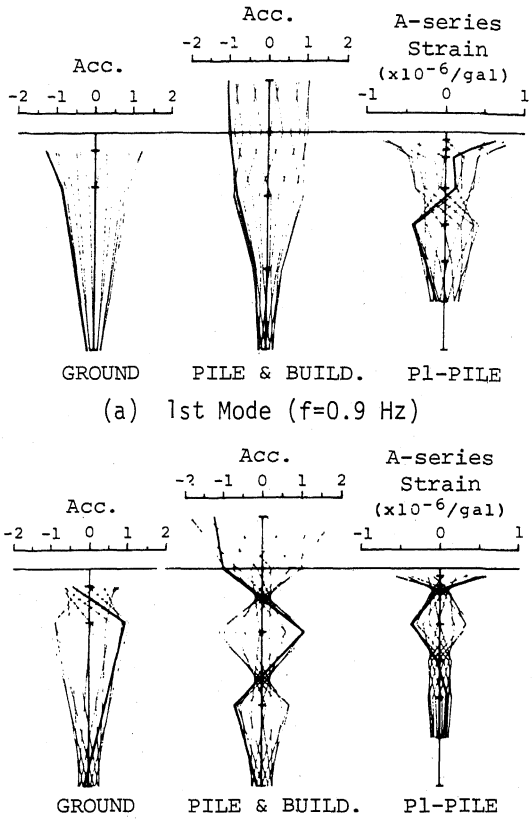

Fig. 12 Normalized Mode Shape (No.33 Earthquake)

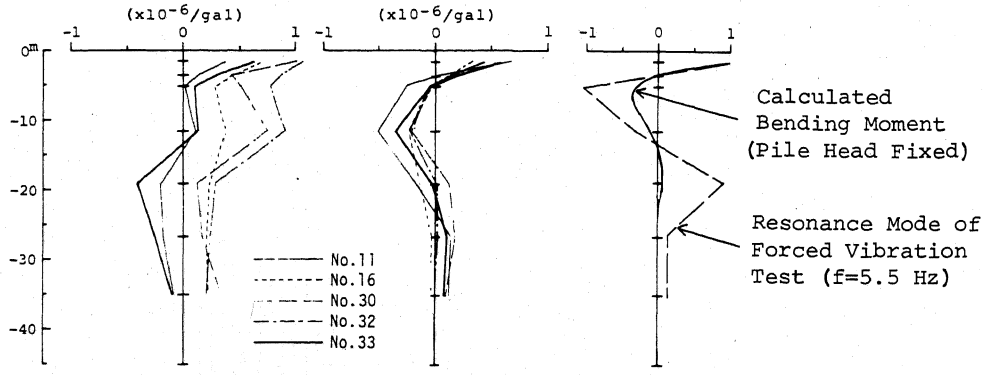

Fig. 13 Normalized Mode Shape of A-series Strain of Pl-pile